JOURNAL OF SUSTAINABLE ENGINEERING AND TECHNOLOGY

Journal homepage: www.joset.com.ng

OPTIMIZING THE INCORPORATION OF PERIWINKLE SHELL FINE AGGREGATE IN HOT-MIX ASPHALT WEARING COURSE

Murana A. A. [1], Eberemu A. O.[2], M. U. Alfa [3], Okpanachi V. U.[4]

1234 Department of Civil Engineering, Ahmadu Bello University Sokoto Road, PMB 06, Zaria, Kaduna state.

ARTICLE INFO

Article History
Received: 18 Oct 2024
Accepted: 07 Feb 2025
Published: 18 April 2025

Corresponding Author:

Victor Udale Okpanachi
Department of Civil Engineering, Ahmadu Bello University Sokoto Road, PMB 06, Zaria, Kaduna state.
Email:
vuokpanachi@acenpee.abu.edu.ng

ABSTRACT

This study seeks to optimize the periwinkle shell content when used as fine aggregate in hot-mix asphalt. The Design-Expert 13 software was used for the optimization process. A custom-designed experiment was carried out and the data set was imported into the software for further analysis. The control design comprised one numeric factor (bitumen content) while the investigation design constituted two numeric factors (bitumen and periwinkle shell fine aggregate content). The responses were the stability, flow, bulk unit weight, voids in the mineral aggregates, air voids in the bitumen content, indirect tensile strength and tensile strength ratio. The models revealed that both factors generally had a significant effect on the HMA responses both individually and interactively, with the periwinkle shells showing more influence. All statistical measures revealed that the models developed showed a good relationship among the variables. The optimum binder content for the control mix was determined to be 6.032% while the optimum contents for the binder and the periwinkle shells were established to be 93.124% and 6.207% for the investigation mix respectively. The scanning electron microscopy of the optimum asphalt mixes confirmed the presence of more voids in the control compared to the investigation.

Keywords: *Periwinkle · shell fine aggregate · Mechanical and volumetric asphalt properties · Optimization ·*

1. Introduction

The features of hot-mix asphalt (HMA) are greatly influenced by the physical, chemical, and mechanical characteristics of the fine aggregate particles [1]. "The shape and surface roughness of fine aggregate has been proven to have an impact on the performance and attributes of asphalt mixtures [2, 3, 4]. The optimum fine aggregate content in HMA is necessary to establish because excess fine aggregate content causes reduced stability and strength, increased moisture susceptibility, increased susceptibility to rutting and permanent deformation, decreased skid resistance, reduced workability, Increased risk of fatigue cracking, higher air voids, segregation, higher binder content and reduced Load-carrying capacity; on the other hand, deficiency in fine aggregates results in reduced workability, increased permeability, susceptibility to ravelling, poor surface texture, inadequate fatigue resistance, and reduced load carrying capacity [5, 6, 7, 8]. Hence, a need to optimize the content of fine aggregates in HMA [9]. The performance properties of pavement that should be optimized are its resistance to loads, ability to rut, frictional qualities, and ability to withstand moisture damage [10, 11]. [12] carried out a study on the potential of glass cullet as fine aggregate in HMA. The result of the study revealed that the optimum glass cullet as fine aggregate in HMA was determined to be 8%. [13] conducted a study on the mechanical characteristics of modified hot mix asphalt using carbonized wood chips (CWP) in place of fine aggregate and polyethene terephthalate (PET) fibres as a binder ingredient. The result of the study revealed that CWP can only replace up to 18% of the weight of fine aggregates at PET levels of 5% and 10%. [14] researched the use of cementitious components as fine aggregate in asphalt mixtures made from construction and demolition debris. The result of the study confirms the feasibility of replacing up to 30% by mass of fine aggregates in HMA.

Periwinkles are particularly valuable in Nigeria's riverine environments. Aside from being eaten, shells from snails are also used for decorations, bead making, poultry bird feed, manufacture of concrete and soil improvement [15]. Each year, approximately twelve (12) million tonnes of periwinkle shells are generated as garbage as a result of the ingestion of the periwinkle marine snail [16]. Calcium oxide (CaO) and Silicon dioxide (SiO_2) are in relative abundance in periwinkle shells among other oxides present [17]. Studies reveal that improvements in the physical properties of HMA have been associated with the presence of CaO and S_iO_2 which help in resisting asphalt pavement failures such as moisture damage, fatigue, rutting, stripping ravelling and bleeding [18, 19]. Therefore, Optimizing the periwinkle shell fine aggregate content in the HMA system not only presents improved performance properties but also is a step in the direction of sustainable construction practice.

2. Materials and Methods /Experimental Program and Analysis

2.1 Methods

Numerical analysis

Numerical analysis was carried out in the form of analysis of variance, property modelling, and optimization using the Design Expert Software version 13.

Experimental design.

The experimental design stage in the software utilizes either the standard designs or the custom design. The standard designs consist of the factorial design, mixture design and the response surface design. The custom design consists of the optimal (combined) design, blank spreadsheet design, importation of already designed data set design, User-defined design, and the simple sample data analysis design allows for varying the input variables at different levels to collect data for the response variable. The importation of an already-designed data set was utilized in this study. The already custom-designed data set comprised the control and the investigation design. The control design comprised one numeric factor (the bitumen content which ranges from 5 – 7% bitumen contents at intervals of 0.5%) and 8 responses as shown in Table 1 (which are the stability, flow, bulk unit weight (ρ_b) per cent air-voids (Pa), voids in mineral aggregates (VMA), voids filled with bitumen (VFB), indirect tensile strength (ITS) and tensile strength ratio (TSR)). The investigation design comprised two numeric factors A and B (the bitumen and the PS content) and the 8 responses. The bitumen content was varied between 5 – 7% at 0.5% intervals and PS content was varied from 0 to 100% at 20% intervals. The trials were carried out for each design point, making a total of 90 runs. The design points or data were imported from the Microsoft Excel datasheet onto the design expert software under the custom design of which further analysis was then carried out.

Table 1: Average values of numerical data for the factors and responses of the HMA.

Bitumen (%)	PS (%)	Stability (kN)	Flow (mm)	ρ_b (kN/m^3)	Pa (%)	VMA (%)	VFB (%)	ITS (kN/m^2)	TSR (%)
5		5.4	3.4	22.819	5.91	17.173	65.59	759.4	60.5
5.5		6.5	3.7	23.346	3.03	15.705	80.71	806.6	62.8
6.0	0	7.7	3.9	23.180	3.02	16.748	81.98	885.2	66.1
6.5		6.4	4.1	23.033	2.94	17.715	83.43	960.6	68.8
7.0		5.5	4.2	22.900	2.80	18.627	84.95	1051.5	71.5
5		6.1	3.0	22.613	6.22	17.383	64.22	698.7	64.2

5.5		7.7	3.4	23.139	3.34	15.904	79.00	751.6	66.8
6.0	20	8.1	3.5	22.986	3.29	16.903	80.55	822.8	69.6
6.5		6.7	3.7	22.840	3.21	17.869	82.02	905.6	72.4
7.0		5.8	3.8	22.692	3.16	18.838	83.24	997.5	74.9
5		6.6	2.9	22.517	6.48	17.598	63.16	862.8	79.1
5.5		8.6	3.1	23.032	3.65	16.156	77.40	915.6	80.3
6.0	40	9.4	3.2	22.893	3.54	17.104	79.28	986.9	81.8
6.5		7.6	3.4	22.714	3.61	18.187	80.14	1069.5	83.2
7.0		5.9	3.7	22.562	3.58	19.170	81.33	1161.5	84.5
5		7.6	2.4	22.403	6.82	17.875	62.01	827.3	87.5
5.5		9.5	2.8	22.894	4.09	16.518	75.20	882.5	88.3
6.0	60	11.2	2.9	22.776	3.90	17.390	78.06	946.8	89.2
6.5		8.4	3.1	22.643	3.78	18.309	79.26	1029.6	90.1
7.0		6.9	3.4	22.490	3.75	19.292	80.93	1006.6	91.4
5		9.6	2.3	22.287	7.17	18.166	60.56	989.2	92.4
5.5		10.6	2.5	22.773	4.46	16.822	73.50	1042.1	92.8
6.0	80	12.4	2.6	22.653	4.28	17.698	75.82	1113.3	93.3
6.5		11.6	2.8	22.521	4.16	18.611	77.65	1196.1	93.7
7.0		8.9	3.1	22.393	4.03	19.506	79.33	1288.0	94.2
5		10.5	2.1	22.222	7.30	18.267	60.04	833.7	96.4
5.5		11.5	2.3	22.705	4.60	16.930	72.81	886.6	96.6
6.0	100	14.3	2.4	22.592	4.40	17.779	75.27	957.8	96.9
6.5		12.6	2.6	22.461	4.28	18.691	77.11	1040.6	97.1
7.0		9.9	3.0	22.333	4.15	19.586	78.79	1132.5	97.4

Development and analysis models

It does this by making use of techniques such as regression analysis (which could be linear or polynomial regression) to fit a mathematical model (often a polynomial equation) to the collected data. This model relates the response variable to the input variables and their interactions. The model typically looks like this:

$$Y = f(x_1, x_2, \ldots, x_n) + \varepsilon \ldots\ldots\ldots (1)$$

where Y is the response variable, and $x_1, x_2, \ldots, x_n$ are the input variables, f is the mathematical function representing the system, and ε represents the error term. These models allow researchers to predict the behaviour of the system within the experimental range of the studied factors.
Once the models are built, they are then analyzed to understand the relationships between the input variables and the responses using statistical techniques like:

- Analysis of variance (ANOVA).
- The R^2 value, Adjusted R^2 value and predicted R^2 value.
- The normal plot of Residuals
- The plot of Residuals versus the Predicted.
- Predicted versus Actual value.

ANOVA

ANOVA helps determine if the model is a good fit for the data. If the model is statistically significant, it can be used for prediction and optimization. ANOVA helps to understand and analyze how the various independent variables, or factors, influence a particular response variable in a designed experiment. It does this by:

i. Determining significance: ANOVA helps determine which factors and interactions significantly affect the response variable. By comparing the variances associated with different factors, ANOVA identifies which factors have a significant impact on the response. In Design-Expert, you can assess the significance of main effects, two-factor interactions, and higher-order interactions.
ii. Partitioning Variability: ANOVA partitions the total variability observed in the response variable into different components attributed to individual factors and their interactions. This partitioning helps researchers understand the relative contributions of each factor and its interaction with the overall variability in the response.

iii. Factor Importance Ranking: The ANOVA table shows the significance levels (p-values) of each factor and interaction. Lower p-values indicate higher significance. By examining these p-values, researchers can rank the importance of factors and interactions. This ranking guides decision-making in refining the experimental setup or focusing on specific factors for further analysis.

iv. Lack of fitness: ANOVA uses the F_{value} and P_{value} by comparing the ratio of mean squares (MS) associated with model variability (SSM) and unexplained variability (SSE). If the MS due to lack of fit (SSE) is significantly larger than the MS due to pure error (residuals within the model), it suggests a lack of fit. The F-$_{value}$ is calculated as $\frac{MSM}{MSE}$, which indicates the ratio of model variability to unexplained variability. A large F-value relative to the critical F-value (based on the chosen significance level) suggests a lack of fit. The associated p-value indicates the probability of observing such a large F-value if the model fits well. A small p-value (<0.05) suggests lack of fit.

The R^2 value, Adjusted R^2 value and predicted R^2 value.

The R^2 measures the proportion of the variance in the dependent variable that is predictable from the independent variables in the model. It ranges from 0 to 1, where 1 indicates a perfect fit. A higher R^2 value suggests that a larger portion of the variance in the dependent variable is explained by the independent variables, indicating a better fit of the model to the data.

The *Predicted R^2* measures how well the model predicts new, unseen data points. It accounts for the number of predictors and the sample size. The predicted R^2 is particularly useful in predicting the model's performance on new data. A higher predicted R^2 indicates a better ability to generalize the model to new observations, indicating good predictive power.

The *Adjusted R^2* adjusts the R^2 value based on the number of predictors in the model. It penalizes the addition of unnecessary predictors that do not significantly improve the model fit. A higher adjusted R^2 indicates a better balance between model complexity (number of predictors) and goodness of fit. It helps prevent overfitting by favouring simpler models with similar or slightly lower R^2 values. The adjusted R^2 value should be significantly close to the predicted R^2 value, in other words, the difference between the two should not be greater than 0.2.

The normal plot of Residuals.

A normal plot, also known as a normal probability plot or Q-Q (quantile-quantile) plot, is a graphical tool used to assess if a set of data follows a normal distribution. In the context of regression analysis and DOE, it can be used to evaluate if the residuals (the differences between observed and predicted values) from the model are normally distributed. A normal probability plot can be interpreted using the terms in the following paragraphs:

i. Ideal Normal Probability Plot: In an ideal normal probability plot, the points follow a straight line, indicating that the residuals are normally distributed. The x-axis represents the theoretical quantiles from a standard normal distribution, and the y-axis represents the observed quantiles from the residuals.

ii. Normal Plot of Residuals for a Well-Fitted Model: If the residuals are normally distributed, the points on the normal probability plot should approximately form a straight line. This suggests that the model fits the data well, and the residuals exhibit a normal distribution.

iii. Normal Plot of Residuals for a Model with Lack of Fit: If the residuals deviate significantly from a straight line and show patterns (such as curvature or outliers), it indicates a lack of fit. Lack of fit means that the model does not capture the underlying data pattern accurately.

The plot of Residuals versus the Predicted.

The plot of residuals versus the predicted values is a common diagnostic tool used to assess the lack of fit in a regression model. This plot helps to identify patterns or trends in the residuals, which can indicate issues with the model's fit. This can be described as follows:

i. Ideal Residuals vs. Predicted Plot: In an ideal scenario, the residuals should be scattered randomly around the horizontal line at zero. This means that there is no pattern or trend in the residuals, indicating a good fit.

ii. Residuals vs. Predicted Plot for a Well-Fitted Model: When the residuals are randomly scattered around the zero line, the model is a good fit. There is no discernible pattern, suggesting the model captures the data well.

iii. Residuals vs. Predicted Plot for a Model with Lack of Fit: When there is a pattern or trend in the residuals, it indicates a lack of fit. Here are a few common patterns and what they suggest:

- ✓ U-Shaped or Inverted U-Shaped Pattern: This indicates a lack of fit, especially if the residuals are large at both low and high predicted values. It suggests the presence of a curvature that the model does not capture.
- ✓ Increasing or Decreasing Trend: An increasing or decreasing trend in the residuals suggests the model is missing a systematic pattern in the data.
- ✓ Fan-Shaped Spread: A fan-shaped spread indicates increasing variance as predicted values increase. It suggests the presence of heteroscedasticity, where the variability of the residual changes across different predicted values.

The plot of Predicted versus Actual values

The plot of Predicted versus Actual (observed) values is a fundamental diagnostic tool in regression analysis. It's especially valuable for assessing the lack of fit in a regression model. The interpretation of the plot is described in the following paragraphs:

- ✓ Ideal Scenario: In an ideal scenario, where the model fits the data perfectly, the actual versus predicted plot should form a perfect diagonal line (y = x). This means that the predicted values match the actual values exactly.
- ✓ Lack of Fit - Underfitting: Underfitting occurs when the model is too simple to capture the complexity of the data. In an actual versus predicted plot for an underfit model:
  - ➢ Points are scattered far away from the diagonal line.
  - ➢ The plot may show a consistent pattern or curvature.
  - ➢ It suggests the model cannot represent the underlying data adequately.
- ✓ Lack of Fit - Overfitting: Overfitting occurs when the model is too complex and fits the noise in the data instead of the underlying pattern.
  - ➢ In an actual versus predicted plot for an overfit model:
    - ▪ The model fits the training data very closely but performs poorly on new, unseen data.
    - ▪ Points might be scattered around the training data points, following the noise.
    - ▪ The model predicts training data well but fails to generalize to new data.
- ✓ Balanced Fit: A well-balanced model captures the underlying pattern without fitting the noise.
  - ➢ In an actual versus predicted plot for a balanced fit:
    - ▪ Points are reasonably close to the diagonal line but might spread out slightly.
    - ▪ There is no consistent pattern or curvature.
    - ▪ The model predicts both the training data and new data reasonably well.

Optimization of the system

Use the response surface model to find the optimal combination of input factors that maximize or minimize the output responses. Optimization can be done using various techniques such as graphical methods, numerical optimization algorithms, or desirability functions. Points inside the design space are assessed using the desirability function. The following criteria were set for the factors A (bitumen content) and B (periwinkle shell content) as well as the responses as shown in Table 2

Table 2 Optimization Goals and Criteria for the Factors and Responses

Factors and Responses	Goals	Lower-Limit	Upper-Limit
Bitumen content	is in range	5	7
Periwinkle shell content	is in range	0	100
Stability	maximize	5.35	14.37
Flow	is in range	2	4
Unit-weight	is in range	22.1977	23.3577
Air-voids	is in range	3	5
VMA	is in range	14	18
VFB	is in range	75	82
ITS	maximize	668.85	1304.09
TSR	maximize	60.15	97.39

The collective desirability (D) is the geometric average of the individual desirability (d_i) of each response.

$$D = (d_1 \times d_2 \times \ldots \times d_n)^{\frac{1}{n}} = \sum_{i=1}^{n} d_i^{\frac{1}{n}} \quad \ldots\ldots\ldots (2)$$

The degree to which the evaluated point matches the response objective determines the individual desirability d_i (which ranges from 0 to 1).

Post-analysis and validation

Sequel to obtaining the optimal solution, the results are then interpreted in the context of the problem domain. Additionally, the validation of the optimized conditions experimentally will also be ensured so that the predicted optimal conditions are practical and feasible.

The validation is achieved by confirming the results obtained by preparing the asphalt mix with optimal solutions provided by the software. The response values obtained from the tests should be within the tolerance limits as stipulated by the software. The confidence level of the tolerance limits was chosen at a 95% confidence level and a 5% significance level. Hence the tolerance high and low limits will fall between the low 95% prediction interval (PI) and the high 95% PI. Each response will have its own 95% PI low and high which the observed value will fall within.

Scanning electron microscopy (SEM).

The SEM was done per [20]. SEM was used to carry out a comparative micro-structural assessment between the optimum control HMA samples prepared with granite quarry fines and the optimum investigation HMA prepared with periwinkle shells fine aggregates.

3. Results and Discussion

3.1 Response surface Models and analysis of Models

The coefficients of the control response surface models developed and the results of the ANOVA carried out on the models to help understand the relationships between the input variables and the responses as well as their fitness/lack of fitness for prediction are presented in Table in Tables 3, 4, 5, 6, 7, 8, 9 and 10.

Table 3: ANOVA of the Stability model

Source	Coefficient	F-value	P-value	Comments
Model		3071.202	<0.0001	Significant
Intercept	4647.310			
A	– 3176.287	53.814	<0.0001	Significant
A^2	808.891	3191.275	<0.0001	Significant
A^3	–90.851	66.004	<0.0001	Significant
A^4	3.798	1556.866	<0.0001	Significant

Table 4: ANOVA of the Flow model

Source	Coefficient	F-value	P-value	Comments
Model		355.71	< 0.0001	Significant
Intercept	– 309.693			
A	208.072	130.08	< 0.0001	Insignificant
A^2	– 51.847	1.03	0.3349	Insignificant
A^3	5.740	0.7923	0.3943	Insignificant
A^4	– 0.238	5.76	0.0373	Significant

Table 5: ANOVA of the Bulk unit-weight model

Source	Coefficient	F-value	P-value	Comments
Model		12.352	0.0012	Significant
Intercept	10.042			
A	4.43	0.453	0.5136	Insignificant
A^2	– 0.372	24.251	0.3349	Insignificant

Table 6 ANOVA of the Air-voids model

Source	Coefficient	F-value	P-value	Comments
Model		442.134	< 0.0001	Significant
Intercept	2948.335			
A	1900.072	12.052	0.006	Insignificant
A^2	– 458.612	2.238	0.1655	Insignificant
A^3	– 49.042	217.908	< 0.0001	Significant
A^4	1.961	30.479	0.0003	Significant

Table 7: ANOVA of the VMA model

Source	Coefficient	F-value	P-value	Comments
Model		393.28	< 0.0001	Significant
	2605.305			
A	– 1678.465	546.125	< 0.0001	Significant
A^2	405.999	2.918	0.1184	Insignificant
A^3	- 43.465	218.542	< 0.0001	Significant
A^4	1.740	32.263	0.0002	Significant

Table 8: ANOVA of the VFB model

Source	Coefficient	F-value	P-value	Comments
Model		624.435	< 0.0001	Significant
Intercept	– 14028.25			
A	9103.481	0.428	0.5277	Insignificant
A^2	– 2197.533	1.880	0.2003	Insignificant
A^3	235.177	197.094	< 0.0001	Significant
A^4	–9.412	28.882	0.0003	Significant

Table 9: ANOVA of the ITS model

Source	Coefficient	F-value	P-value	Comments
Model		726.252	< 0.0001	Significant
Intercept	861.064			
A	– 141.107	1439.124	< 0.0001	Significant
A^2	24.061	13.381	0.0033	Significant

Table 10: ANOVA of the TSR model

Source	Coefficient	F-value	P-value	Comments
Model		1069.469	< 0.0001	Significant
A	5.575	1069.469	< 0.0001	Significant
A^2	32.494		0.0033	Significant

The result of the coefficients of the investigation response surface models and ANOVA carried out on the models are shown in Tables 11, 12, 13, 14, 15, 16, 17 and 18.

Table 11: ANOVA of the investigation Stability model

Source	Coefficient	F-value	P-value	Comments
Model		312.854	< 0.0001	Significant
Intercept	9.94			
A	-0.3752	4.37	0.0397	Significant
B	3.56	409.63	< 0.0001	Significant
AB	0.0315	0.1498	0.6998	Insignificant
A^2	-7.23	172.03	< 0.0001	Significant
B^2	2.43	27.84	< 0.0001	Significant
A^2B	-0.7548	30.06	< 0.0001	Significant
B^2A	0.4318	9.59	0.0027	Significant
A^3	-0.0563	0.0921	0.7623	Insignificant
B^3	-0.4418	5.58	0.0207	Significant
A^4	4.09	69.55	< 0.0001	Significant

B^4	-1.48	12.76	0.0006	Significant
Lack of fit		211.69	< 0.0001	Insignificant

Table 12: ANOVA of the investigation Flow model

Source	Coefficient	F-value	P-value	Comments
Model		1201.46	< 0.0001	Significant
Intercept	3.07			
A	0.2962	160.38	< 0.0001	Significant
B	-0.8229	1119.54	< 0.0001	Significant
AB	0.0170	2.21	0.1408	Insignificant
A^2	0.0060	0.2101	0.6479	Insignificant
B^2	-0.0554	0.7366	0.3933	Insignificant
A^2B	0.1321	47.04	< 0.0001	Insignificant
A^3	0.1441	30.83	< 0.0001	Significant
B^3	0.0581	4.92	0.0293	Significant
B^4	0.1541	7.04	0.0096	Significant
Lack of fit		7.68	< 0.0001	Insignificant

Table 13: ANOVA of the investigation Air-voids model

Source	Coefficient	F-value	P-value	Comments
Model		267.26	< 0.0001	Significant
Intercept	3.39			
A	0.0559	0.1621	0.6883	Insignificant
B	0.4092	73.07	< 0.0001	Significant
A^2	0.0832	0.0329	0.8564	Insignificant
A^3	-1.58	104.91	< 0.0001	Significant
A^4	1.29	10.03	0.0021	Significant
Lack of fit		1.21	0.2727	Insignificant

Table 14: ANOVA of the investigation bulk unit-weight model

Source	Coefficient	F-value	P-value	Comments
Model		255.44	< 0.0001	Significant
Intercept	22.81	169.07		
A	-0.3831	827.50	< 0.0001	Significant
B	-0.2920	0.6390	< 0.0001	Significant
A^2	0.0777	17.86	0.4264	Insignificant
B^2	0.0734	167.59	< 0.0001	Significant
A^3	0.4231	21.64	< 0.0001	Significant
A^4	-0.4023	169.07	< 0.0001	Significant
Lack of fit		1.12	0.3557	Insignificant

Table 15: ANOVA of the investigation VMA model

Source	Coefficient	F-value	P-value	Comments
Model		1442.65	< 0.0001	Significant
Intercept	16.89			
A	2.29	4054.83	< 0.0001	Significant
B	0.2713	196.81	< 0.0001	Significant
AB	-0.1700	10.40	0.0018	Significant
A^2	-0.3198	7.25	0.0086	Significant
B^2	0.0666	9.83	0.0024	Significant
A^2B	-0.0375	1.60	0.2097	Insignificant
A^3	-1.58	1558.27	< 0.0001	Significant
A^3B	0.1305	4.98	0.0285	Significant

A^4	1.51	204.38	< 0.0001	Significant
Lack of fit		0.9618	0.5177	Insignificant

Table 16: ANOVA of the investigation VFB model

Source	Coefficient	F-value	P-value	Comments
Model		267.26	< 0.0001	Significant
Intercept	80.01			
A	1.33	42.17	< 0.0001	Insignificant
B	-2.36	462.76	< 0.0001	Significant
AB	0.1540	2.39	0.1261	
A^2B	1.06	2.48	0.1194	Insignificant
A^3	0.5074	9.07	0.0035	Significant
A^4	8.19	1300.88	< 0.0001	Significant
Lack of fit		1.59	0.0799	Insignificant

Table 17: ANOVA of the investigation ITS model

Source	Coefficient	F-value	P-value	Comments
Model		267.26	< 0.0001	Significant
Intercept	980.13			
A	149.85	301.01	< 0.0001	Significant
B	248.36	97.84	< 0.0001	Significant
B^2	-43.36	8.03	0.0057	Significant
B^3	-201.60	48.20	< 0.0001	Significant
Lack of fit		26.53	< 0.0001	Insignificant

Table 18: ANOVA of the TSR model

Source	Coefficient	F-value	P-value	Comments
Model		4095.26	< 0.0001	Significant
Intercept	86.23			
A	2.55	319.01	< 0.0001	Significant
B	21.48	6352.62	< 0.0001	Significant
AB	-3.95	107.23	< 0.0001	Significant
B^2	-18.13	556.49	< 0.0001	Significant
B^2A	0.6083	6.86	0.0105	Significant
B^3	-5.97	366.60	< 0.0001	Significant
AB^3	1.36	9.56	0.0027	Significant
B^4	13.31	370.44	<0.0001	Significant
Lack of fit		3.23	0.0002	Insignificant

The result of the tables above reveals that most of the terms in the models developed have a significant impact on their respective responses. Hence it can be inferred that the factors both individually and interactively statistically have a significant effect on the responses of both the control and investigation asphalt mixes.

The lack of fit assessment revealed that the models developed (besides the flow model) exhibited an insignificant lack of fit results. An insignificant lack of fit result is good; it shows that the model, to a significant degree, describes the behaviour and interaction of the responses and their respective factors. This trend observed is synonymous with the study carried out by [21, 22].

R^2 value, Adjusted R^2 value and predicted R^2 value.

The values of the R^2, Adjusted R^2 and predicted R^2 for the control and the investigation response models developed are shown in Tables 19 and 20

Table 19: R^2, Adjusted R^2 and predicted R^2 values of the control responses

Responses	Stability	Flow	Unit-weight	Air-voids	VMA	VFB	ITS	TSR
R^2	0.999	0.993	0.673	0.994	0.994	0.996	0.992	0.988
Adjusted R^2	0.999	0.990	0.619	0.992	0.991	0.994	0.990	0.987
Predicted R^2	0.998	0.984	0.529	0.987	0.986	0.991	0.988	0.985
Adjusted R^2 _ Predicted R^2	< 0.2	< 0.2	< 0.2	< 0.2	< 0.2	< 0.2	< 0.2	< 0.2

Table 20: The R^2, Adjusted R^2 and predicted R^2 values of the investigation responses

Responses	Stability	Flow	Unit-weight	Air-voids	VMA	VFB	ITS	TSR
R^2	0.978	0.993	0.949	0.941	0.994	0.996	0.841	0.998
Adjusted R^2	0.975	0.992	0.945	0.937	0.993	0.996	0.833	0.997
Predicted R^2	0.971	0.991	0.941	0.933	0.992	0.995	0.825	0.997
Adjusted R^2 _ Predicted R^2	< 0.2	< 0.2	< 0.2	< 0.2	< 0.2	< 0.2	< 0.2	< 0.2

The results of the R^2, and adjusted R^2 values of both the control and investigation models as shown in the Tables are significantly higher than average. This implies that a high proportion of the variance in the responses can be predicted from the factors in the model. In simpler terms, the factors explain the variation observed in the responses to a relatively high degree. It should be noted that adjusted R^2 values are adjustments of the R^2 values for the excesses emanating from the factors. In other words, it penalizes the tendency for the R^2 values to increase due to the number of factors (predictors) present in the models. This trend observed is synonymous with the study carried out by [21, 22].

The values of the predicted R^2, which is also relatively higher than average, imply that the degree to which the model's prediction will fit into (or describe) new and unseen data is relatively higher than average. In other words, Unlike the regular R^2 value, which quantifies the proportion of variance explained in the sample data used to build the model, the predicted R^2 estimates how well the model is expected to perform on new, future data points. The difference between the adjusted and the predicted R^2 values for all the responses was found to be within the acceptable limit of <0.2. This trend observed is synonymous with the study carried out by [21, 22].

The normal plot of residuals.

The normal plot of residuals of the control and investigation responses are shown in Figures 1, 2, 3, 4, 5, 6, 7, 8, 9, 10, 11, 12, 13, 14, 15 and 16.

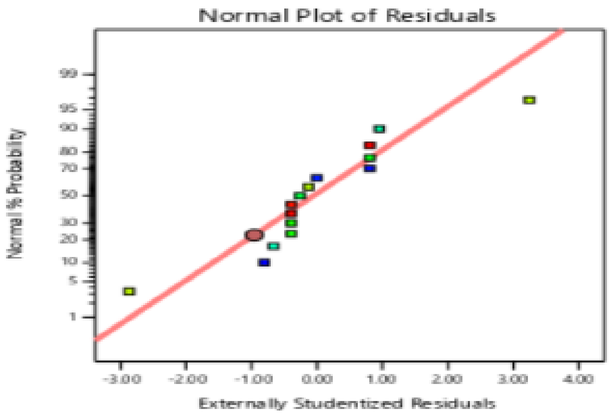

Figure 1: Stability plot (control).

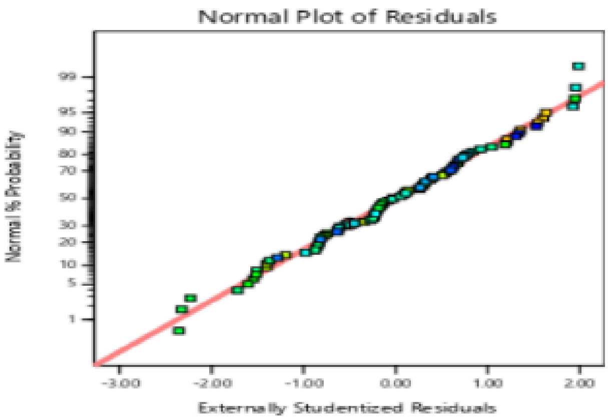

Figure 2: Stability plot (Investigation).

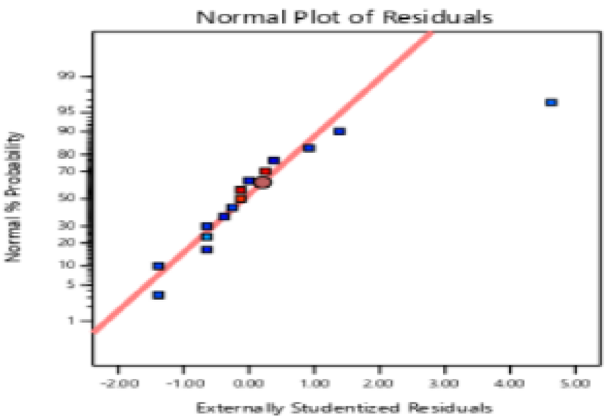

Figure 3: Flow plot (Control).

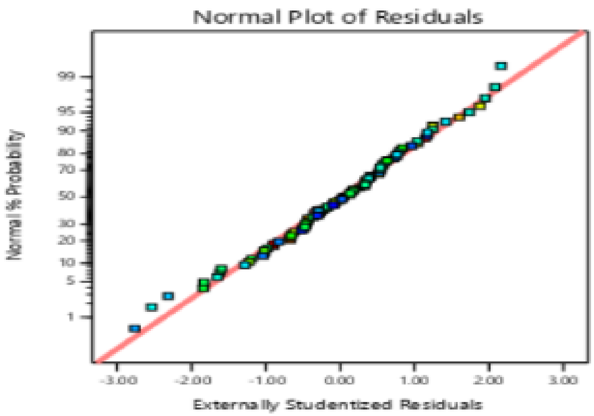

Figure 4: Flow plot (investigation).

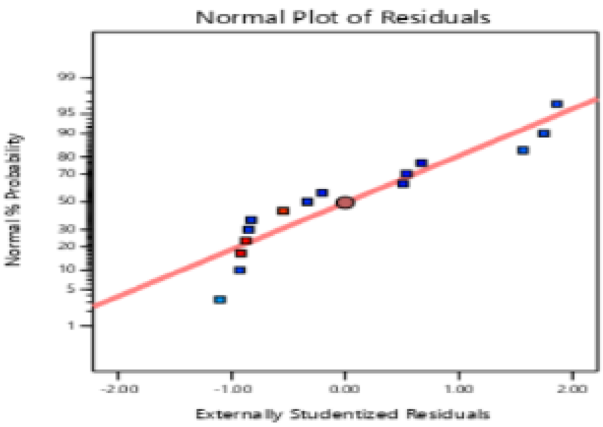

Figure 5: Unit-weight plot (Control).

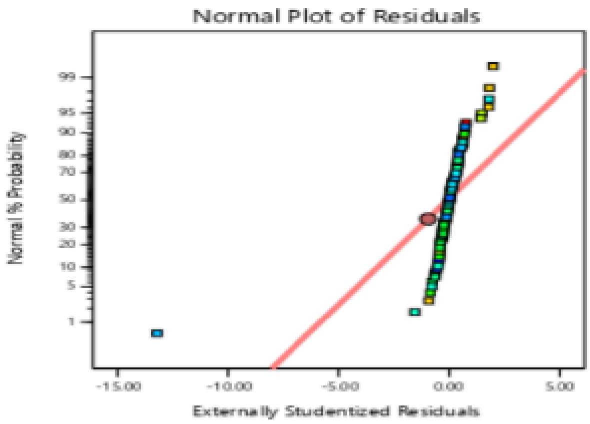

Fig 6: Unit-weight plot (Investigation).

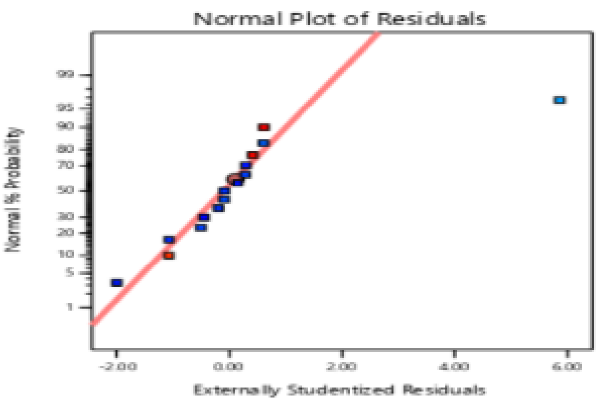

Figure 7: Air-voids plot (Control).

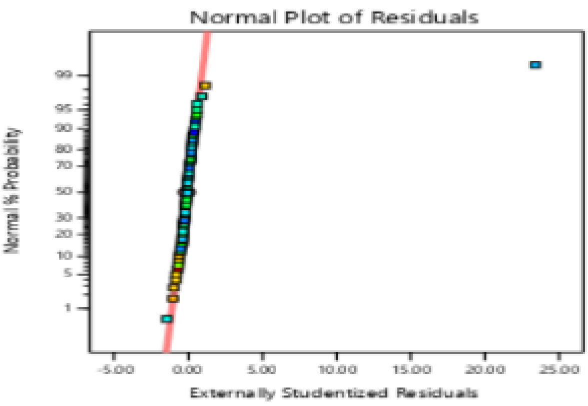

Figure 8: Air-voids plot (Investigation).

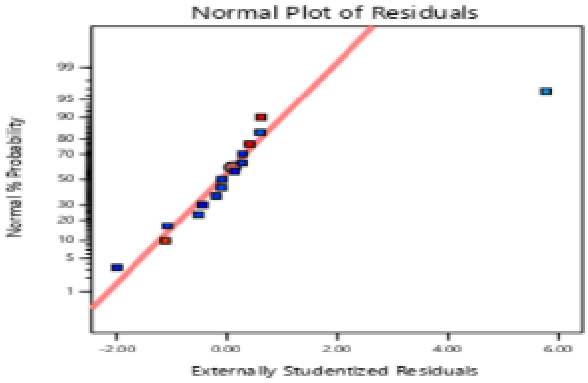

Figure 9: VMA plot (Control).

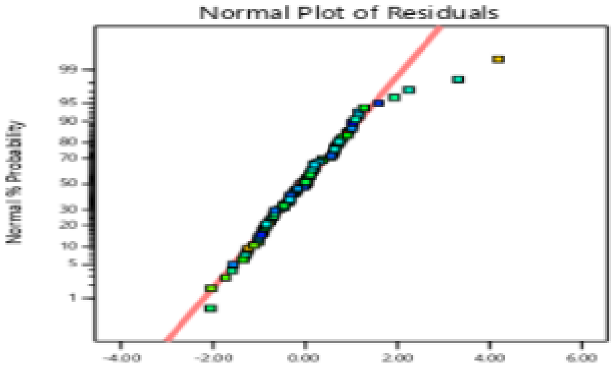

Figure 10: VMA plot (Investigation).

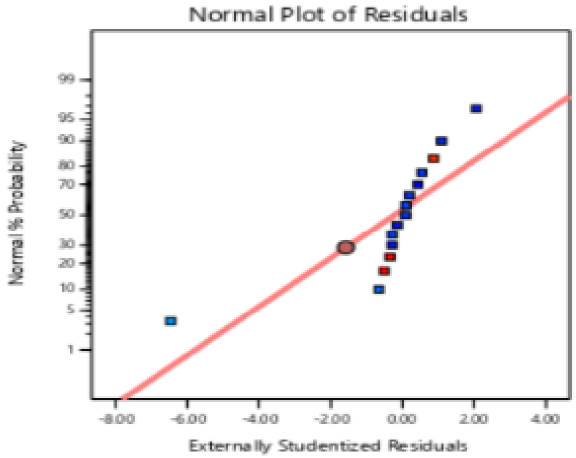

Figure 11: VFB plot (Control).

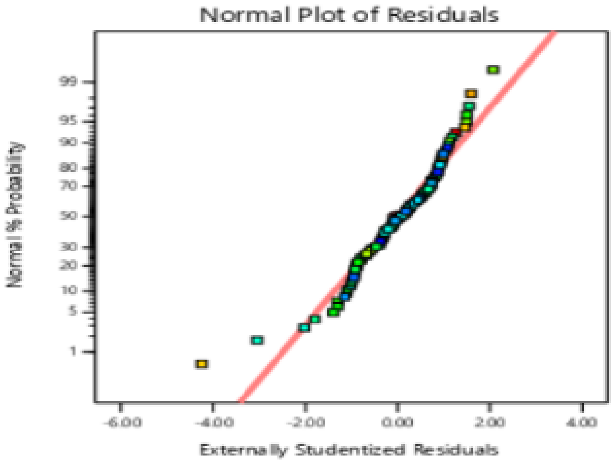

Figure 12: VFB plot (Investigation).

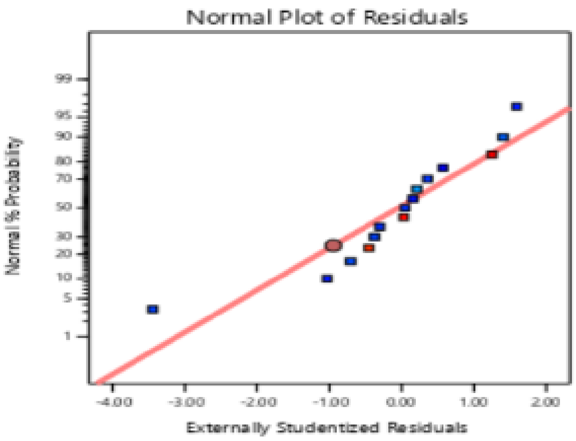

Figure 13: ITS plot (Control).

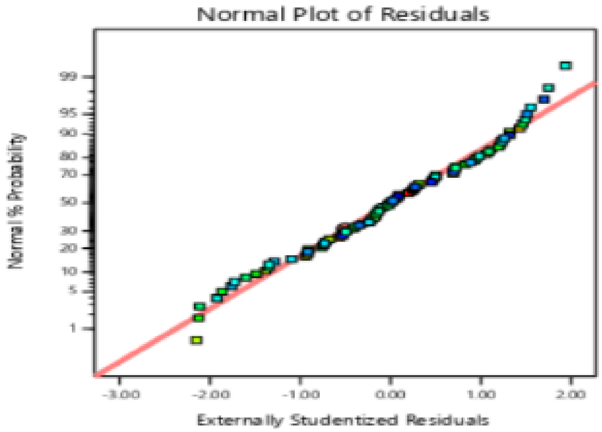

Figure 14: ITS plot (Investigation).

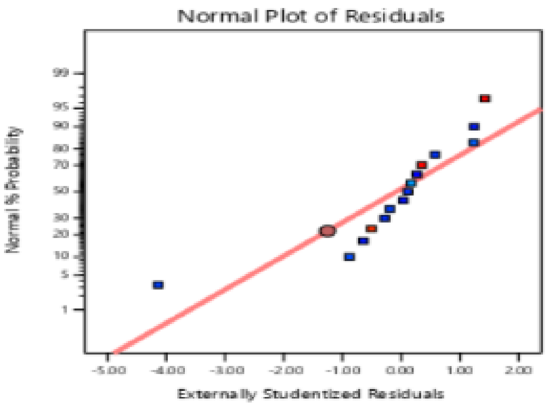

Figure 15: TSR plot (Control).

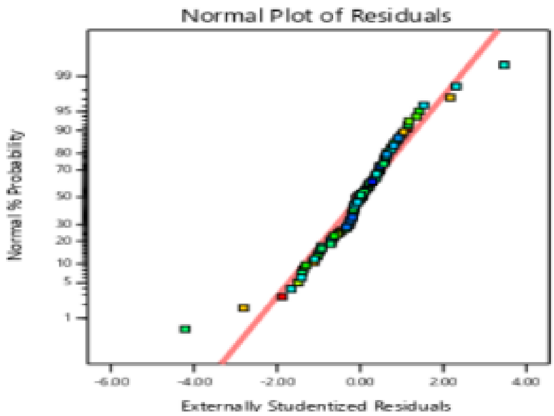

Figure 16: TSR plot (Investigation).

As shown by the Figures, the normal probability plot of residuals is normally distributed. These can be observed by how the points on the normal probability plot approximately or closely form a straight line. This suggests that the model fits the data well, and the residuals exhibit a normal distribution. This trend is observed generally for all the responses for both the control and the investigation. This trend observed is synonymous with the study carried out by [23, 24].

The plot of residuals versus predicted.

The plot of residuals versus predicted of the control and investigation responses are as shown in Figures 17, 18, 19, 20, 21, 22, 23, 24, 25, 26, 27, 28, 29, 30, 31 and 32.

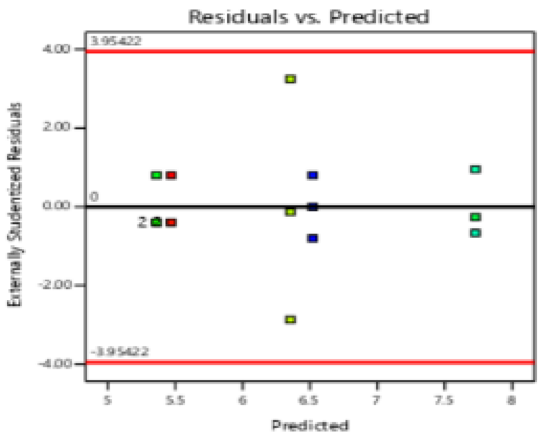

Figure 17: Stability plot (Control).

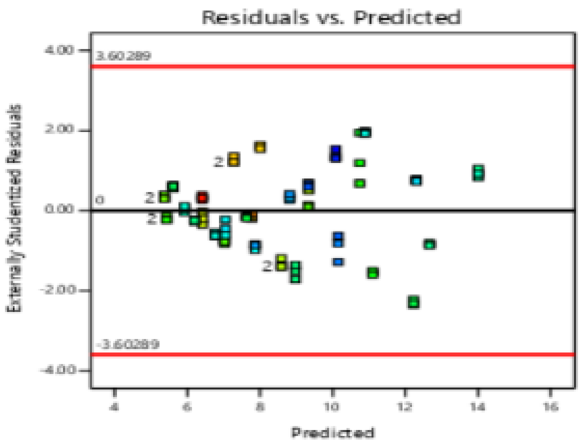

Figure 18: Stability plot (Investigation).

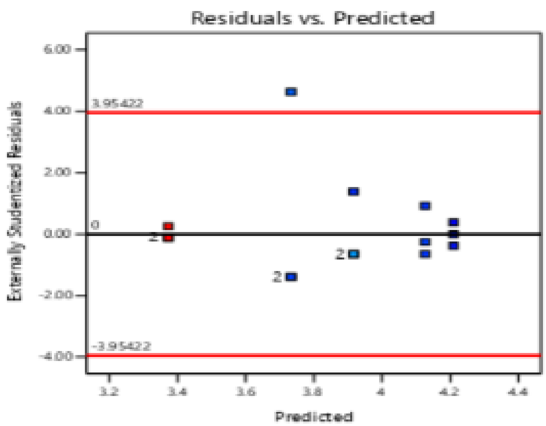

Figure 19: Flow plot (Control).

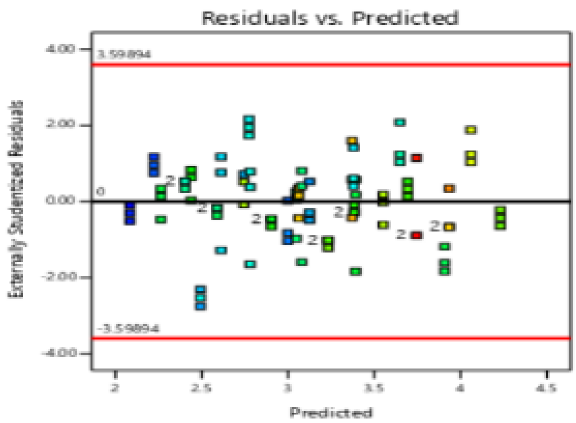

Figure 20: Flow plot (Investigation).

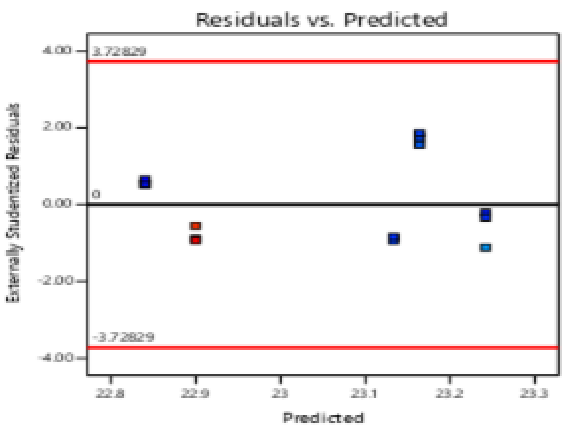

Figure 21: Unit-weight plot (Control).

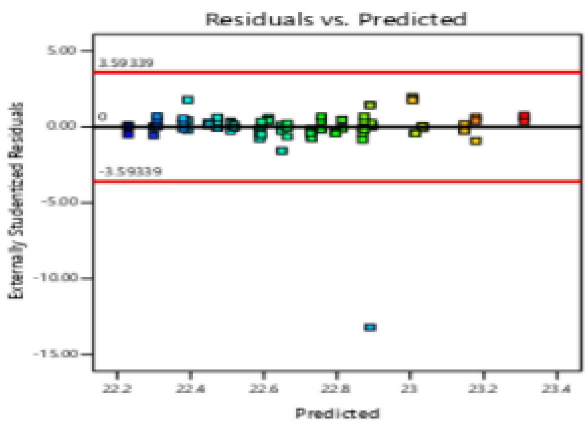

Figure 22: Unit-weight plot (Investigation).

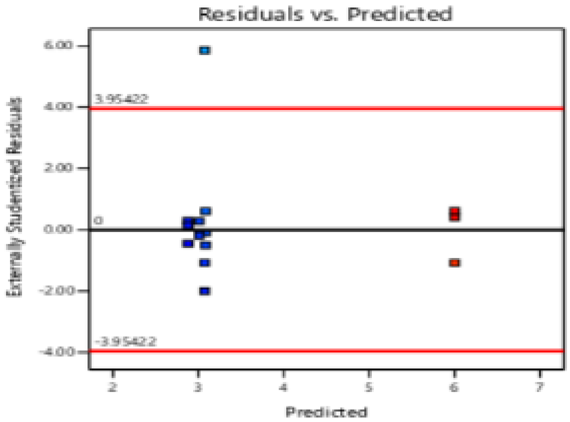

Figure 23: Air-voids plot (Control).

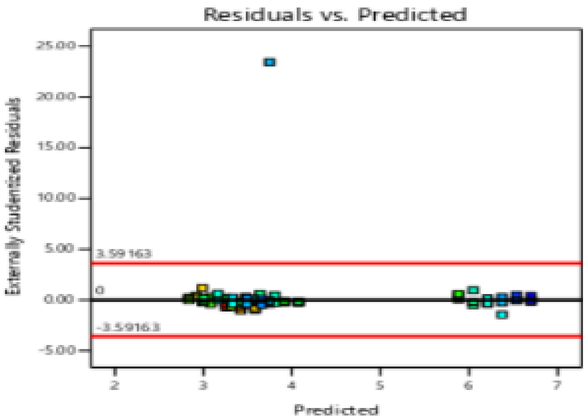

Figure 24: Air-voids plot (Investigation).

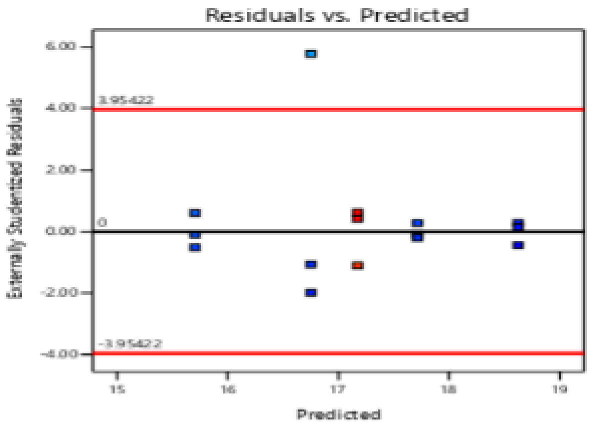

Figure 25: VMA plot (Control).

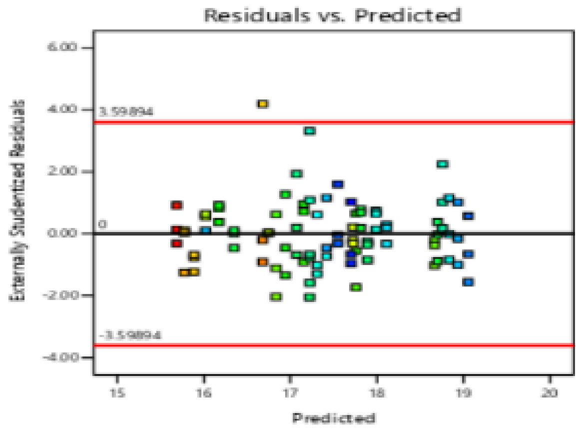

Figure 26: VMA plot (Investigation).

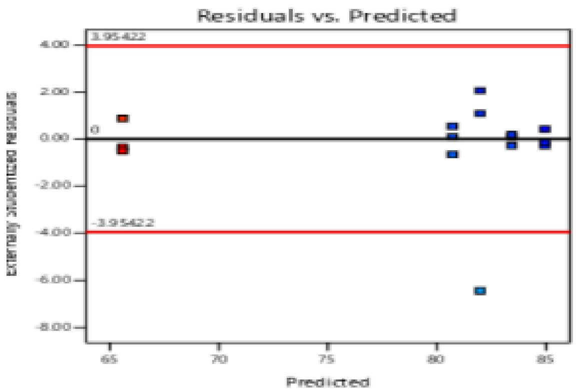

Figure 27: VFB plot (Control).

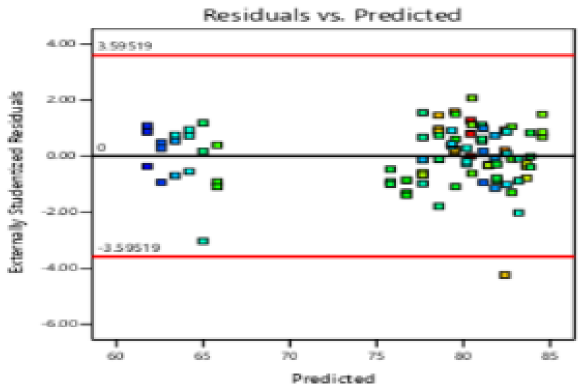

Figure 28: VFB plot (Investigation).

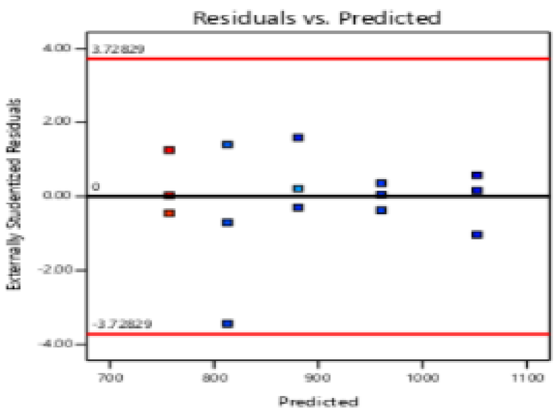

Figure 29: ITS plot (Control).

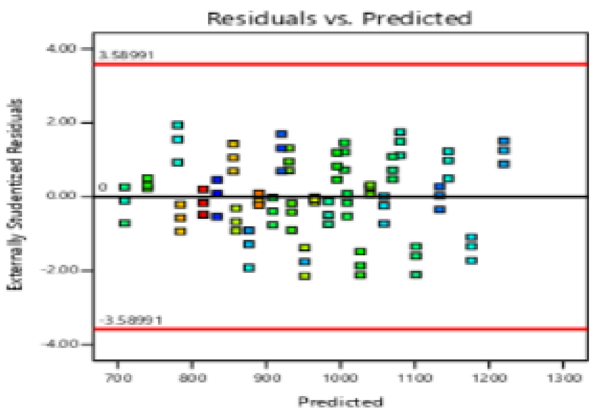

Figure 30: ITS plot (Investigation).

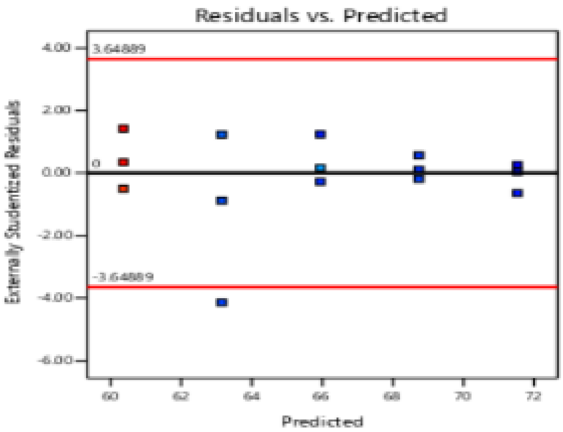

Figure 31: ITS plot (Control).

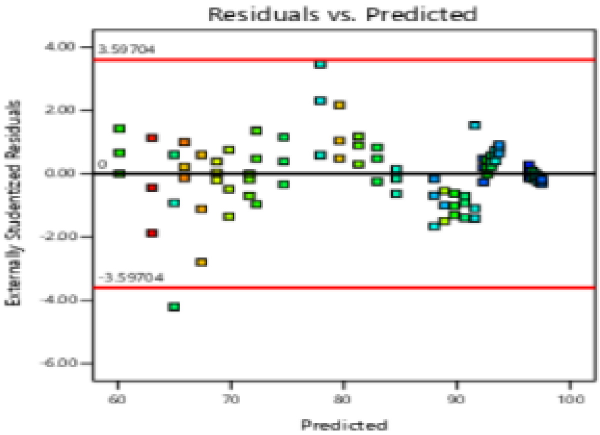

Figure 32: ITS plot (Investigation).

A careful observation of the residual versus predicted plots of all the responses reveals randomly scattered points around the horizontal line at zero. This means that there is no pattern or trend in the residuals, indicating a good fit or a low degree lack of fit. This trend observed is synonymous with the study carried out by [21, 22].

The predicted versus actual plot.

The cook distance plot of the control and investigation responses are shown in Figures 33, 34, 35, 36, 37, 38, 39, 40, 41, 42, 43, 44, 45, 46, 47, and 48.

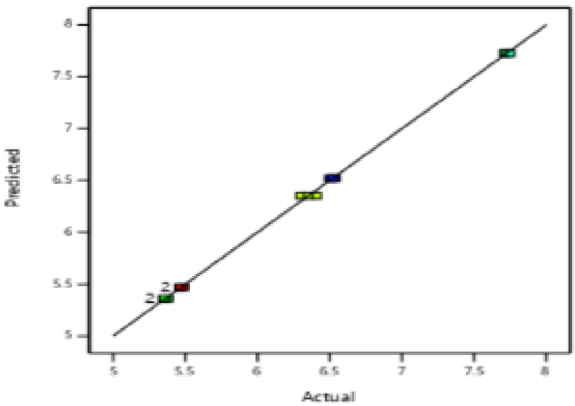

Figure 33: Stability plot (Control).

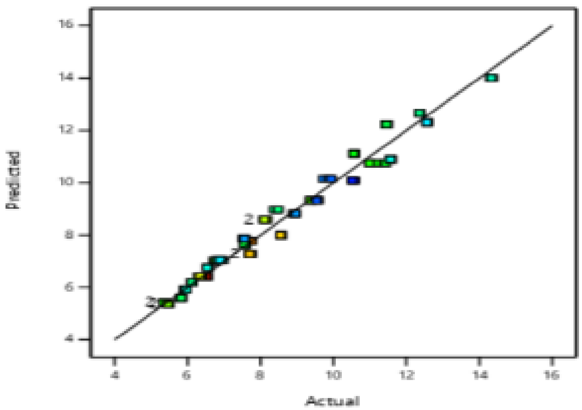

Figure 34: Stability plot (Investigation).

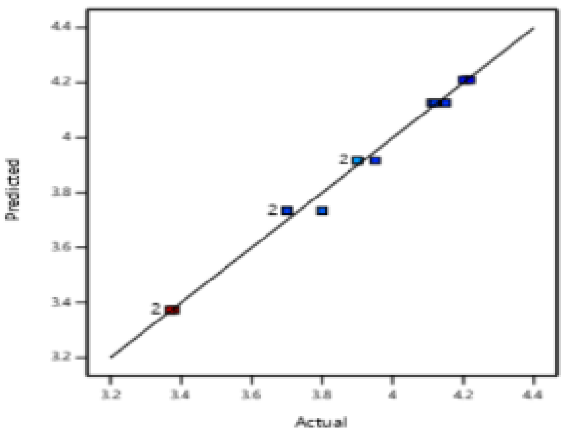

Figure 35: Flow plot (Control).

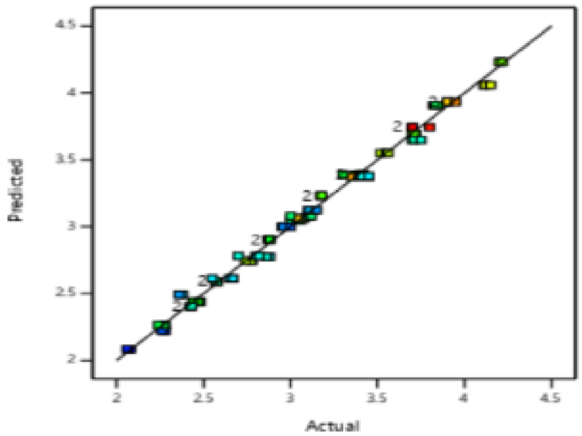

Figure 36: Flow plot (Investigation).

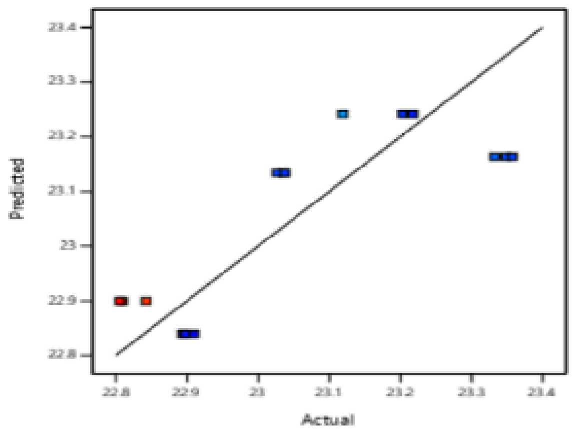

Figure 37: Unit-weight plot (Control).

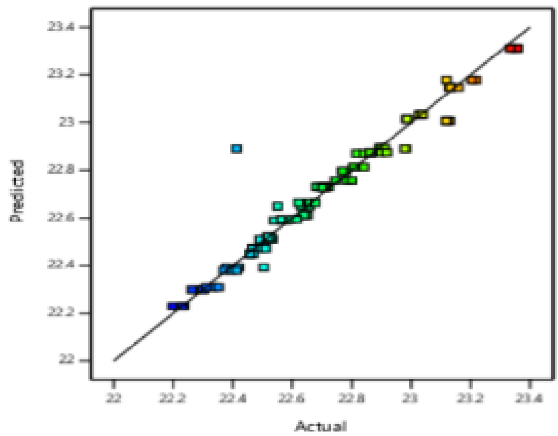

Figure 38: Unit-weight plot (Investigation).

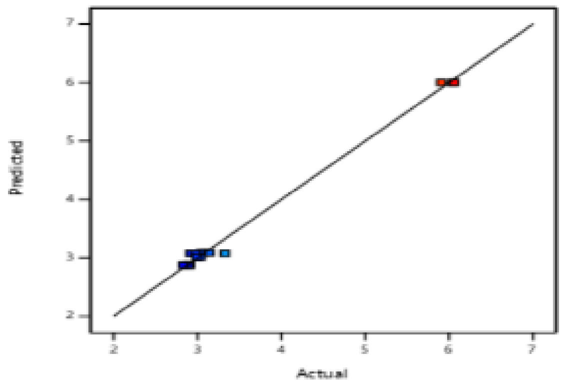

Figure 39: Air-voids plot (Control).

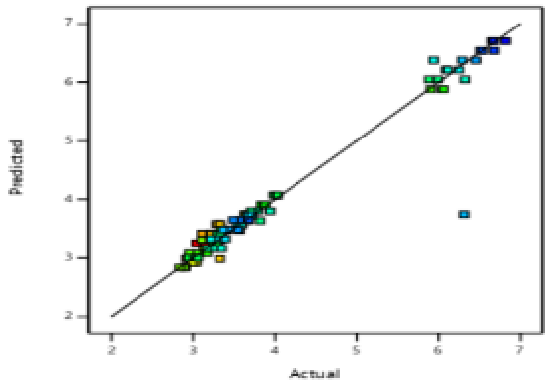

Figure 40: Air-voids plot (Investigation).

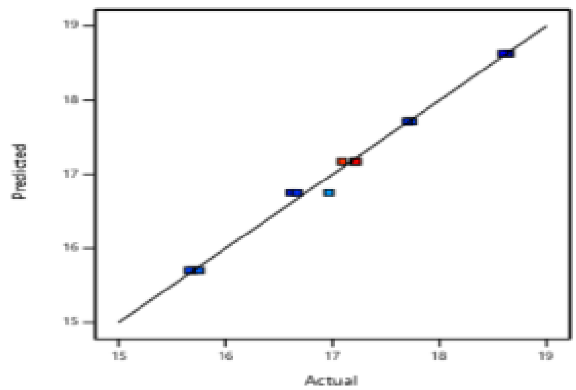

Figure 41: VMA plot (Control).

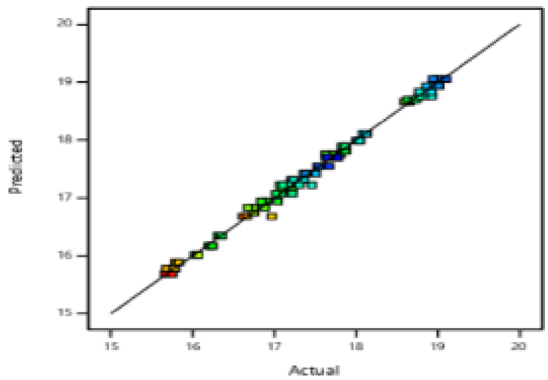

Figure 42: VMA plot (Investigation).

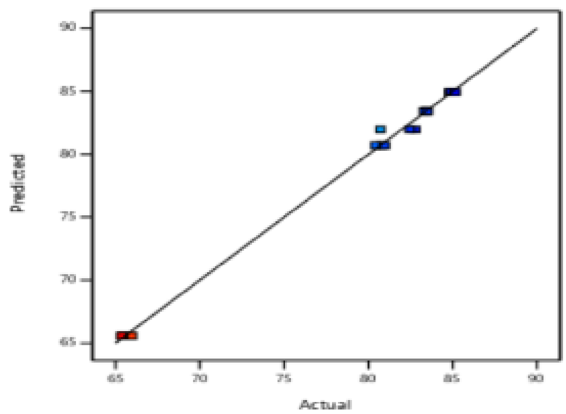

Figure 43: VFB plot (Control).

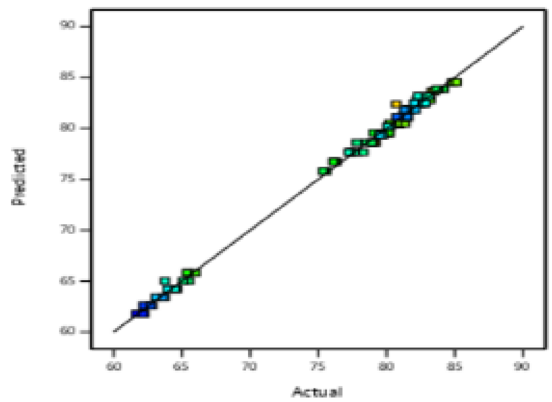

Figure 44: VFB plot (Investigation).

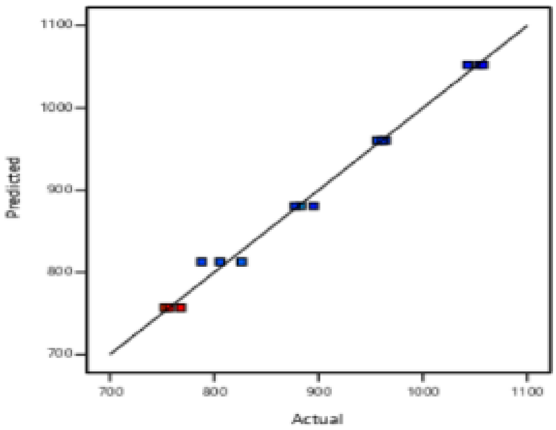

Figure 45: ITS plot (Control).

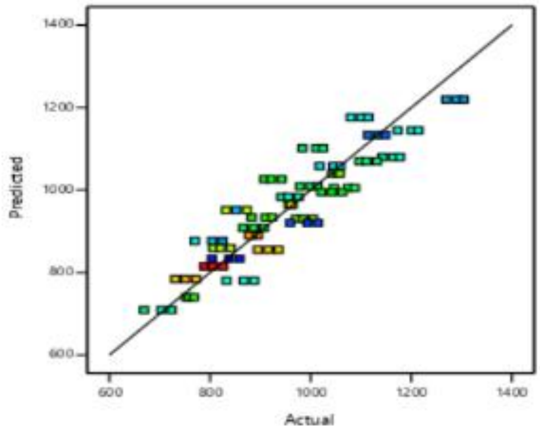

Figure 46: ITS plot (Investigation).

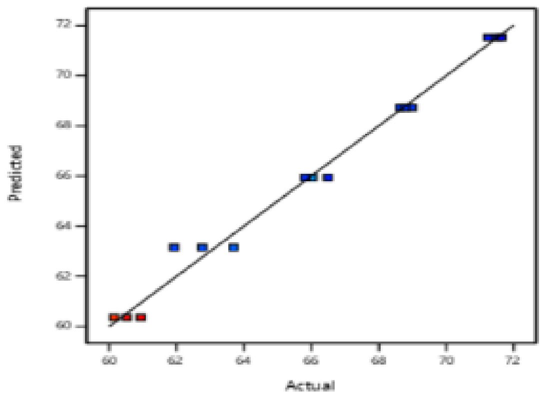

Figure 47: ITS plot (Control).

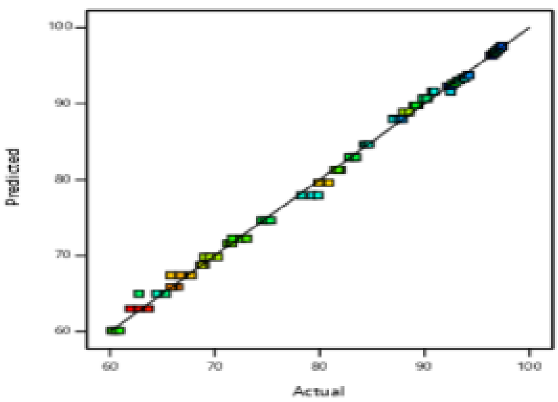

Figure 48: ITS plot (Investigation).

The plots of the actual versus the residuals for the control and investigation responses as depicted by the figures above show the data points are arranged linearly around a perfect diagonal line (y = x) of the rectangular plot area. This means that the predicted values match the actual values exactly. This trend observed is synonymous with the study carried out by [21, 22].

3.2 Optimization

The result of the optimum solutions for the responses of both the control and the investigation asphalt mixes are presented in Table 21

Table 21: Optimization solutions

Factors, Responses and Desirability	Control	Investigation
Bitumen content (A)	6.032	6.207
Periwinkle shells content (B)	--	93.194
Stability	7.713	13.385
Flow	3.929	2.512
Bulk unit-weight	23.24	22.542
Air-voids	3.088	3.751
VMA	16.825	17.589
VFB	82	78.396
ITS	885.333	1063.416
TSR	66.119	94.917
Desirability	0.786	0.802

As observed in Table 21 the optimum values of the responses of the investigation are better than those of the control. A 73.54% improvement is observed in the stability values, a 20.114% improvement in the ITS is also observed, and a 43.55% improvement in the TSR values. These values imply that the investigation material (periwinkle shell fine aggregates material) was able to improve the rutting, fatigue and moisture susceptibility under the improvements recorded in the stability, ITS and TSR values. However, a slight increment in bitumen content of 2.9% was observed. This may be attributed to the higher void contents present in the investigation HMA compared to the control HMA. The solutions presented relatively higher than average desirability. This trend observed is synonymous with the study carried out by [23].

3.3 Model Validation

The results of the observed response optimum values of both the control and the investigation asphalt mix obtained by laboratory testing of the asphalt mix produced from the optimum conditions (of the values of factors A and B from Table 20) as determined by the design expert software are as shown in Table 22 and 23. These observed values are also compared to the optimum values predicted through optimization.

Table 22: Control Model validation

Responses	Predicted mean	Observed	95% PI Low	95% PI High
Stability	7.713	7.703	7.636	7.790
Flow	3.929	3.99	3.850	4.008
Bulk unit-weight	23.24	22.498	22.953	23.527
Air-voids	3.088	3.269	2.804	3.371
VMA	16.825	16.873	16.581	17.070
VFB	82	82.388	80.602	83.398
ITS	885.333	889.312	860.306	910.359
TSR	66.119	66.666	65.077	67.1601

Table 23: Investigation Model validation

Responses	Predicted mean	Observed	95% PI Low	95% PI High
Stability	13.385	13.532	12.603	14.168
Flow	2.512	2.508	2.403	2.621
Bulk unit-weight	22.542	22.498	22.407	22.677
Air-voids	3.751	3.815	3.115	4.387
VMA	17.589	17.573	17.421	17.757
VFB	78.396	78.388	77.450	79.342
ITS	1063.416	1063.412	946.161	1180.672
TSR	94.917	93.991	93.646	96.190

A comparison between the optimum laboratory observed values with the 95% high/low prediction confidence interval and the optimum predicted mean reveals that the differences between observed values and the predicted values are negligible and within acceptable limits. Furthermore, the observed values fall within the range of the high and low 95% confidence prediction interval. This trend observed is synonymous with the study carried out by [21, 22].

3.4 Scanning Electron Microscopy.

The result of the SEM carried out on the optimum control and investigation asphalt mixes are as presented in Plates 1 and 2

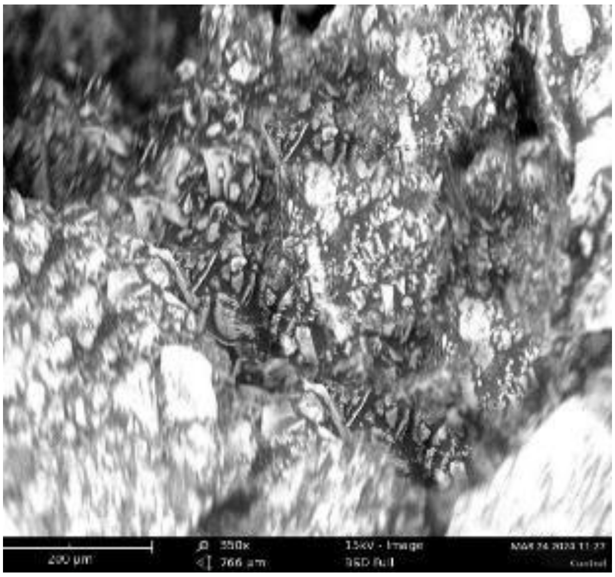

Plate 1: SEM image of the control HMA

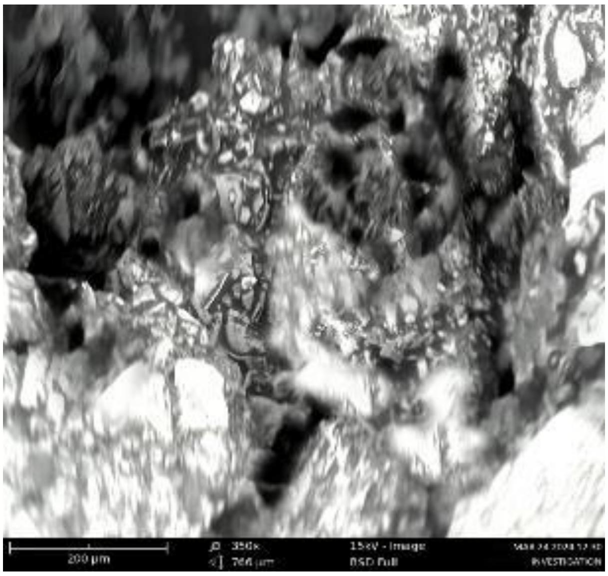

Plate 2: SEM image of the investigation HMA

The SEM images of the control and the investigation are similar. However, the presence of more voids can be observed (by the visible black spots in the images) in the investigation HMA when compared to the control HMA. These images concur with the findings observed in the general trend of the void properties of both the control/investigation HMA samples (as shown in Table 21). This trend observed is synonymous with the study carried out by [24].

4. Conclusions

The conclusions drawn from the study are summarized in the following paragraphs:

1. The ANOVA carried out on the terms of the models developed revealed that both factors generally had a significant effect on the HMA responses both individually and interactively. However, the PS showed a higher influence on the responses in comparison to the binder. Furthermore, other statistical evaluating measures such as the R^2, adjusted R^2, predicted R^2, the difference between the adjusted and the predicted R^2, the normal plot or residuals, residuals versus predicted plot and the predicted versus actual value plot all showed that the models developed were valid to describe the relationship between factors and the responses effectively.

2. The quantity of PS content and bitumen content required to yield optimum responses was established to be 93.124% and 6.207% respectively. The optimum binder content for the control mix was determined to be 6.032%. The laboratory post-analysis carried out to validate the optimum values revealed the observed values of the responses fell within the range of the high and low 95% confidence prediction interval. In addition, the comparative micro-structural study between the optimum control and investigation asphalt mixes revealed that the investigation possessed more voids in comparison to the control HMA.

5. References

[1] I. Kamruddin, M. B. Napiah, and Y. G. Alkhalig, "The Effect of Fine Aggregate Properties on The Rutting Behaviour of the Conventional and Polymer Modified Bituminous Mixtures Using Two Types of Sand as Fine Aggregate," in Proceeding of Malaysian Universities Transportation Research Forum and Conferences, Universiti Tenaga Nasional, 2010, p. pp 89-98.

[2] A. Topal and B. Sengoz, "Determination of Fine Aggregate Angularity in Relation with the Resistance to Rutting of hot-mix Asphalt," Construction and Building Materials, vol. 19, no. 2, pp. 155–163, Mar. 2005, doi: https://doi.org/10.1016/j.conbuildmat.2004.05.004.

[3] E. Masad, D. Olcott, T. White, and L. Tashman, "Correlation of Fine Aggregate Imaging Shape Indices with Asphalt Mixture Performance," Transportation Research Record: Journal of the Transportation Research Board, vol. 1757, no. 1, pp. 148–156, Jan. 2001, doi: https://doi.org/10.3141/1757-17.

[4] R. P. Chapuis and P. P. Legare, A Simple Method for Determining the Surface Area of Fine Aggregate and Filler in Bituminous Mixtures, Effect of Aggregates and Mineral Filler on Asphalt Mixture Performance, vol. ASTM STP 1147. Philadelphia: American Society for Testing and Materials, 1992.

[5] N. Khan et al., "Effect of Fine Aggregates and Mineral Fillers on the Permanent Deformation of Hot Mix Asphalt," Sustainability, vol. 15, no. 13, p. 10646, Jan. 2023, doi: https://doi.org/10.3390/su151310646.

[6] J. Ji et al., "Effect of Water Absorption and Loss Characteristics of Fine Aggregates on Aggregate-Asphalt Adhesion," KSCE Journal of Civil Engineering, vol. 25, no. 6, pp. 2020–2035, Mar. 2021, doi: https://doi.org/10.1007/s12205-021-1464-0.

[7] Alexis Jair Enríquez-León, T. Delgado, F. Thiago, M. Brabo, and Liebert Parreiras Nogueira, "Characterization of the air void content of fine aggregate matrices within asphalt concrete mixtures," Construction & Building Materials, vol. 300, pp. 124214–124214, Sep. 2021, doi: https://doi.org/10.1016/j.conbuildmat.2021.124214.

[8] G. Valdes-Vidal, A. Calabi-Floody, E. Sanchez-Alonso, and R. Miró, "Effect of Aggregate Type on the Fatigue Durability of Asphalt Mixtures," Construction and Building Materials, vol. 224, pp. 124–131, Nov. 2019, doi: https://doi.org/10.1016/j.conbuildmat.2019.07.064.

[9] H. Sivilevičius, V. Podvezko, and S. Vakrinienė, "The Use of Constrained and Unconstrained Optimization Models in Gradation Design of Hot Mix Asphalt Mixture," Construction and Building Materials, vol. 25, no. 1, pp. 115–122, Jan. 2011, doi: https://doi.org/10.1016/j.conbuildmat.2010.06.050.

[10] J. Hu, T. Ma, T. Yin, and Y. Zhou, "Foamed warm mix asphalt mixture containing crumb rubber: Foaming optimization and performance evaluation," Journal of Cleaner Production, vol. 333, pp. 130085–130085, Dec. 2021, doi: https://doi.org/10.1016/j.jclepro.2021.130085.

[11] Fabrizio Meroni, W. Xue, G. W. Flintsch, and B. K. Diefenderfer, "Impact of Mix Design Optimization on HMA Rutting Performance Under Accelerated Pavement Testing," Lecture Notes in Civil Engineering, pp. 108–117, Jan. 2020, doi: https://doi.org/10.1007/978-3-030-55236-7_12.

[12] H. M. Alhassan, G. H. Yunusa, & D. Sanusi (2018). Potential of Glass Cullet as Aggregate in Hot Mix Asphalt. Nigerian Journal of Technology, 37(2), 338. https://doi.org/10.4314/njt.v37i2.8

[13] N. Jegatheesan, T. M. Rengarasu & W. M. K. R. T. W. Bandara (2020). Mechanical Properties of Modified Hot Mix Asphalt Containing Polyethylene Terephthalate Fibers as Binder Additive and Carbonized Wood Particles as Fine Aggregate Replacement. Asian Transport Studies, 6, 100029. https://doi.org/10.1016/j.eastsj.2020.100029.

[14] D. Z. A. Al Hassanieh, G. R. Chehab, I. Srour, & H. A. Kassem, (2016). Recycling Cementitious Constituents of Construction Demolition Waste in Asphalt mixes: the Case of Lebanon. International Journal of Sustainable Society, *8*(2), 109. https://doi.org/10.1504/ijssoc.2016.077513.

[15] O. Ambali, Y. L. Shuaib-Babata, H. K. Ibrahim, L. B. Abdulqadir, N. I. Aremu, and T. O. Ibraheem, (2020). "Production of Abrasive Sandpaper using Periwinkle Shells and Crab Shells". International Journal of Engineering Materials and Manufacture, volume 5, issue 2, pp55-61.

[16] U. G. Eziefula, G. C. Obiechefu, and M. E. Charles (2020) "Use of periwinkle shell by-products in Portland cement-based materials: an overview". International Journal of Environment and Waste Management, Volume 26, Issue 3, pp 362 – 388.

[17] A. Oparaeli, K. Ichechi, M. Oju, Igwe, A. Enwuso, (2020) "Contributions of Periwinkle Shell Ash on the Stability and Elastic Properties of Modified Asphalt Concrete for a High Trafficked Road" International Journal of Constructive Research in Civil Engineering (IJCRCE) Volume 6, Issue 2, pp 1-10 ISSN 2454-8693.

[18] A. Fareed, S.A.B. Zaidi, N. Ahmad, I. Hafeez, A. Ali, M. F. Ahmad (2020) "Use of agricultural waste ashes in asphalt binder and mixture: A sustainable solution to waste management" Construction and Building Materials Volume 259 pp 1-15. Elsevier.

[19] Khodary, F., Abd El-sadek, M.S., El-Sheshtawy, H.S., (2015) "CaO/Bitumen Nanocomposite: Synthesis and Enhancement of Stiffness Properties for Asphalt Concrete Mixtures" International Journal of Scientific & Engineering Research, Volume 6, Issue 1, pp 444-448.

[20] ASTM E986 – 04, Standard Practice for Scanning Electron Microscope Beam Size Characterization. West Conshohocken, PA: ASTM International., 2024.

[21] A. Jiménez del Barco Carrión, A. Subhy, M. A. Izquierdo Rodriguez, and D. Lo Presti, "Optimisation of Liquid Rubber Modified Bitumen for Road Pavements and Roofing Applications," Construction and Building Materials, vol. 249, p. 118630, Jul. 2020, doi: https://doi.org/10.1016/j.conbuildmat.2020.118630.

[22] W. Rafiq et al., "Modeling and design optimization of reclaimed asphalt pavement containing crude palm oil using response surface methodology," Construction and Building Materials, vol. 291, pp. 123288–123288, Jul. 2021, doi: https://doi.org/10.1016/j.conbuildmat.2021.123288.

[23] G. Ruiz, F. P. Chávez, S. Santamaría, W. Araujo, J. Timaná, and R. Schmitt, "Laboratory Evaluation of Seashells Used as Fine Aggregate in Hot Mix Asphalt," International Journal of Pavement Engineering, vol. 21, no. 5, Apr. 2020, doi: https://doi.org/10.1080/10298436.2018.1502435.

[24] J. Zhu, T. Ma, J. Fan, Z. Fang, T. Chen, and Y. Zhou, "Experimental Study of High Modulus Asphalt Mixture Containing Reclaimed Asphalt Pavement," Journal of Cleaner Production, vol. 263, pp. 121447–121447, Aug. 2020, doi: https://doi.org/10.1016/j.jclepro.2020.121447.